Materials and Design 106 (2016) 454–462

Contents lists available at ScienceDirect

Materials and Design

journal homepage: www.elsevier.com/locate/matdes

Dielectric silicone elastomers filled with *in situ* generated polar silsesquioxanes: Preparation, characterization and evaluation of electromechanical performance

Adrian Bele, Mihaela Dascalu, Codrin Tugui, Mihail Iacob, Carmen Racles, Liviu Sacarescu, Maria Cazacu *

Department of Inorganic Polymers, "Petru Poni" Institute of Macromolecular Chemistry, Aleea Gr. Ghica Voda 41 A, Iasi 700487, Romania

ARTICLE INFO

Article history:
Received 14 March 2016
Received in revised form 30 May 2016
Accepted 3 June 2016
Available online 5 June 2016

Keywords:
Intelligent materials
Polymer-matrix composites
Dielectric elastomers
Electro-mechanical actuation
Silicones

ABSTRACT

Dielectric silicone elastomers able to respond to an electrical stimulus by a mechanical displacement are prepared through a simple one-pot procedure consisting in cross-linking and simultaneous *in situ* generation of the filler functionalized with polar groups, as reinforcing and dielectric permittivity enhancer. One and the same reagent, (3-chloropropyl)trimethoxysilane (CPTMS), serves as both cross-linker and precursor for the filler. This is incorporated in different amounts with dibutyltindilaurate (DBTDL) into polydimethylsiloxane-α,ω-diols having molecular masses of 34,500 and 125,000 $g \cdot mol^{-1}$ and left for curing in atmospheric conditions. The Fourier Transform Infrared (FTIR) spectra show absorption bands characteristic for silsesquioxane (SSQ) structures formed by converting excess CPTMS, while the Transmission Electron Microscopy (TEM) images reveal biphasic morphology of the resulting material in which formations which we have assumed to be SSQ are distributed within the silicone matrix. The structural aspects and supramolecular organization are investigated by Wide Angle X-Ray Diffraction (WAXD) and Small Angle X-ray Scattering (SAXS) analysis. The influence of the CPTMS amount over the mechanical and dielectric properties of the resulted materials are investigated expecting an improvement of the dielectric permittivity but also a strengthening of material. Lateral strain as a response to an applied voltage on dielectric films is measured.

1. Introduction

Polydimethylsiloxanes (PDMSs), due to characteristics of the siloxane bond, offer a unique combination of properties (high flexibility, extremely low transition temperatures, high temperature and chemical resistance, hydrophobicity, *etc.*), which are desirable for many applications [1,2]. Besides polyurethanes and acrylic elastomers, silicones are of high interest as dielectric elastomers (DEs) [3] for electromechanical applications due to their high elasticity, high dielectric strength, low moisture uptake, the ability to function in a broad temperature range without significant change in their properties and the capability to be processed into thin flexible films [4]. However, since the intermolecular forces in PDMS are extremely weak, in order to obtain a durable elastomeric material with dimensional stability, it should be cross-linked. In general, three curing procedures are commonly used in silicones chemistry, each with advantages and disadvantages: condensation (moisture cure), addition (hydrosilylation cure), or radical reaction, which is performed normally at higher temperatures [5–7]. The condensation curing is one of the most important procedure used to cross-link siloxanes in commercial applications. Although it requires a longer curing time this is the simplest and cheapest pathway occurring at room temperature without involving expensive reagents or catalysts, and affording thermally stable materials [5]. A typical system contains silanol-terminated PDMS, a cross-linker and a catalyst. Tri- and tetraalkoxysilanes enable moisture-cure capability upon exposure to air, being the most commonly used cross-linkers. The alkoxy functionality is hydrolyzed to form silanol and the corresponding alcohol. The silanol can then condense with the SiOH-terminated PDMS and produce a network. Tin carboxylates are suitable catalysts for this reaction [8]. When a trialkoxysilane is used as cross-linking agent, the fourth organic group attached to the silicon atom, depending on its nature, can induce or develop certain properties. When this is a polar group, it may lead, *inter alia*, to increased dielectric permittivity of silicones, which is required for electromechanical applications.

Because silicones have the disadvantage of a low dielectric permittivity, a significant research effort has been devoted to improve their dielectric permittivity. Several approaches are reported in the literature, mainly consisting in chemical modification of the polysiloxane chains with polar groups [9–14], interpenetration of silicone networks with more polar ones [15–18] or incorporation of polar fillers within silicone matrix [3,9,19–26], each with its limits and performance as were recently reviewed in ref. [27]. The use of polar cross-linkers is less approached, although this may present some strength, consisting of a relatively

---

* Corresponding author.
E-mail address: mcazacu@icmpp.ro (M. Cazacu).

http://dx.doi.org/10.1016/j.matdes.2016.06.010
0264-1275/

uniform distribution of polar groups, their position in the network being dictated by the polymer chain length and polydispersity. To increase the content of polar groups, one can add trialkoxysilane in excess leading to the *in situ* formation of silsesquioxane structures, which, besides contribution to increasing of dielectric permittivity of the material, can play the role of reinforcing filler for the silicone matrix, as described in several literature reports [12,28]. Thus, α,ω-bis(H)-polydimethylsiloxane of relatively low molecular masses (28,000 and 6000 g/mol) were cross-linked by hydrosilylation with triallyloxysilane having attached different sophisticated polar groups and a poly(dimethylmethylvinyl)siloxane as additional crosslinker. An increase of 20–35% in dielectric permittivity was reported for low dipol contents [12,28].

In our previous work [29] we used as cross-linkers some easy accessible, commercially available trialkoxysilanes having different stable organic groups attached to the silicon atom: methyl, 3-chloropropyl, 3-aminopropyl, 3-cyanopropyl and phenyl in a fixed amount, 1.5 ml for 10 g PDMS, irrespective of the molecular weight of cross-linker and of PDMS to be cross-linked (34,500 and 125,000 g/mol). Because the best electromechanical results were obtained for the lower mass PDMS cross-linked with chloropropyltrialkoxysilane, in this paper, we proposed to deepen the study of the effect of this cross-linker. The same polymers were used but varying the cross-linker amounts in a larger range, between 0.10 to 49.12 wt%, as compared to just 16.35 wt% used in our previous work. The mechanical and dielectric characteristics of the prepared materials were evaluated and electromechanical actuation was measured. We propose here an interdisciplinary study involving chemistry of some materials designed and optimized for electromechanical applications (actuation).

2. Experimental

2.1. Materials

Two polydimethylsiloxane-α,ω-diols, PDMSs, having molecular masses, M_n, 34,500 g·mol^{-1}, PDI = 1.5 (A), and 125,000 g·mol^{-1}, PDI = 1.38 (B), respectively as were estimated by Gel Permeation Chromatography, were synthesized by cationic ring-opening polymerization of octamethylcyclotetrasiloxane in the presence of a cation exchanger as catalyst [30]. A α,ω-bis(trimethylsiloxy)polydimethylsiloxane of a molecular mass, Mn, 50,000 g·mol^{-1} was prepared by the same procedure as PDMS-α,ω-diols but in presence of hexamethyldisiloxane as a chain blocking agent. Dibutyltindilaurate, DBTDL, (95%) and (3-chloropropyl)trimethoxysilane, CPTMS, (≥97%) were purchased from Sigma Aldrich and used as received.

2.2. Measurements

Fourier Transform Infrared (FTIR) spectra were recorded on a Bruker Vertex 70 FTIR spectrometer in the transmission mode in the range 400–4000 cm^{-1} at room temperature with a resolution of 2 cm^{-1} and accumulation of 32 scans.

Stress–strain measurements were performed on a Zwick Z010 tensile test machine with a crosshead speed of 200 mm min^{-1}. Tensile test specimens with a gauge width of 2 mm and a gauge length of 18 mm were prepared by die cutting. The strain was determined using a traverse moving sensor. The curves were averaged from three independent experiments. The tensile modulus was determined from the slope of the stress-strain curves using a linear fit to the data points within 10% strain.

Transmission electron microscopy (TEM) analysis have been performed with a HT7700 HITACHI microscope operated in high contrast mode at 100 kV accelerating voltage. The samples were prepared by direct deposition of solid gels particles on 300 mesh holey carbon grids (Ted Pella).

Wide Angle X-Ray Diffraction (WAXD) was performed on a D8 ADVANCE Diffractometer (Bruker AXS, Germany), using the Cu-Kα radiation (λ = 0.1541 nm), a parallel beam with Gobel mirror and a Dynamic Scintillation detector. The working conditions were 40 kV and 30 mA, 2 s/step, 0.02°/step. All the diffractograms were investigated in the range 3–50°, 2 theta degrees, at room temperature.

X-ray scattering was performed using the Nanostar U-Bruker system. The instrument is equipped with a X-ray IμS microsource and a Vantec 2000 detector (diameter of 200 mm). The wavelength of the incident X-ray beam is λ = 1.54 Å (Cu Kα) and the beam is collimated by three pinholes. The sample-to-detector distance was 107 cm allowing measurements with the q values between 0.01 Å^{-1} and 0.15 Å^{-1}. The angular scale was calibrated by the scattering peaks of a silver behenate standard. The samples were measured under vacuum at constant temperature, 25 °C for 4000 s. The empty beam background was subtracted from the original intensity profiles. The data analysis was done using the software SAXS-NT [*Bruker AXS software*].

The dielectric constant measurements were conducted on a Novocontrol Alpha-A Frequency Analyzer using a Hewlett Packard 16451B Dielectric test fixture as electrodes. Shielded electrodes with a diameter of 10 mm were used and the sample thickness was determined using the built in micrometer screw.

Actuation tests were performed using circular film actuators, for which the films were fixed between two circular frames of 25 mm. Circular electrodes (8 mm diameter) of carbon black powder, were applied to each side of the film. A FUG HCL-35-12500 high voltage source served as power supply for actuator tests. The voltage was increased by 100 V every 2 s. The actuation strain was measured optically as the extension of the diameter of the electrode area *via* a digital camera, using an edge detection tool of a LabView program to detect the boundary between the black electrode area and brighter film.

2.3. Preparation of silicone elastomers: A and B series

PDMS (typically 3 g) was dissolved in 5 ml toluene, then cross-linking agent ((3-chloropropyl)trimethoxysilane) and the catalyst (DBTDL) were sequentially added in amounts shown in Table 1, with vigorous stirring for about 5 min after each addition. The viscous solution was cast on Teflon substrate by doctor blade technique and maintained at 25 °C and atmospheric humidity (around 60%). After 24 h, the films were easily removed from the substrate, and kept in laboratory environment for two weeks before measurements were done.

2.4. Preparation of model samples A_5-G, A_{15}-G and A_{50}-G

The as obtained cross-linked materials were not suitable for certain investigations, such as TEM or FTIR in the transmission mode. In order

Table 1
Feed reagents amounts and estimated polar group contents in the cross-linked films.

Sample/Reactants	PDMS, A or B, g	DBTDL, g	CPTMS		wt% Cl[a]
			g	wt%	
A_0	3.000	0.053	0.012	0.391	0.068
A_5	3.000	0.053	0.165	5.127	0.933
A_{10}	3.000	0.053	0.325	9.621	1.777
A_{15}	3.000	0.053	0.474	13.439	2.519
A_{50}	3.000	0.107	3.000	49.124	10.587
B_0	3.000	0.053	0.003	0.098	0.016
B_5	3.000	0.053	0.157	4.891	0.887
B_{10}	3.000	0.053	0.311	9.425	1.704
B_{15}	3.000	0.053	0.465	13.218	2.476
B_{50}	3.000	0.107	3.000	49.124	10.586

[a] Dipole content expressed as wt% Cl was estimated assuming the total conversion of CPTMS to corresponding fully condensed SSQ, $Cl(CH_2)_3SiO_{1.5}$. The following formula was used: wt% Cl $= 100[m_{CPTMS} \times 35.5 / 198.72]/[m_{PDMS} + m_{DBTDL} + m_{CPTMS} \times 129.5 / 198.72]$, with: m_{CPTMS}, m_{PDMS}, m_{DBTDL} – amounts of CPTMS, PDMS and DBTDL, respectively; 198.72 – molecular weight for CPTMS; 129.5 – molecular weight for fully condensed silsesquioxane derivative; 35.5 – atomic mass for chlorine.

to get model systems as close as possible to the silicone elastomers under study, we prepared three samples with similar composition as A_5, A_{15} and A_{50}, but using a trimethylsiloxy-ended PDMS, α,ω-bis(trimethylsiloxy)polydimethylsiloxane, instead of OH-terminated PDMS, polydimethylsiloxane-α,ω-diols. Thus, the cross-linking is not possible, while the amounts of cross-linker and catalyst are the same as in the corresponding cured materials. These samples were labelled as A_5-G, A_{10}-G and A_{50}-G, respectively.

3. Results and discussions

Two polydimethylsiloxane-α,ω-diols, PDMSs, of different molecular weights, Mn (34,500 $g \cdot mol^{-1}$ and 125,000 $g \cdot mol^{-1}$, respectively) were cross-linked with (3-chloropropyl)trimethoxysilane, CPTMS. This was incorporated into the polymer in amounts close to those calculated according to the stoichiometry of the crosslinking reaction (samples A_0 and B_0) or in increasing weight percentages of around 5, 10, 15 and 50 wt% reported to the mixture weight (samples A_5–A_{50} and B_5–B_{50}). In the first phase, the CH_3O-Si groups of CPTMS condense with the Si-OH chain ends of the PDMS in the presence of DBTDL catalyst producing polymer cross-linking. Over time, as the air moisture diffuses inside the polymeric film, the CH_3O-Si groups of excess CPTMS hydrolyze. The resulted triol is instable and it will undergo rapid condensation reactions with itself or with methoxysilane groups. The resulted products are silsesquioxanes, which can have totally or partially condensed skeletal structures: closed (POSS) or open (OPOSS) polyhedral oligomeric silsesquioxane cage, ladder (LSSQ) or random (RSSQ) [31]. These structures will have polar chloropropyl groups, with a dipole moment of 2.86 D (estimated using HyperChem TM), attached to the silicon atoms. Simultaneous occurrence of the two processes that lead to connecting PDMS chains to the silsesquioxane structures acting as cross-linking nodes is also possible. The presumed chemical processes are schematically shown in Scheme 1.

3.1. FTIR analysis

Since it is difficult to register IR spectra for cross-linked silicone films in transmission mode, while ATR spectra show only characteristic bands for PDMS, model samples A_5-G and A_{50}-G were analyzed (Fig. 1a and b). Thus, IR spectra of the two samples reveal large bands in the range 1225–930 cm^{-1} consisting in several overlapping bands [32,33]. The main two bands are those at 1022 and 1094 cm^{-1} (Fig. 1a) or 1018 and 1097 cm^{-1} (Fig. 1b) specific for siloxane bond from long chains of α,ω-bis(trimethylsiloxy)polydimethylsiloxane, which is the major component in the mixture. However, a careful analysis of the spectrum from Fig. 1b permits to identify a series of bands that could be assigned to SSQ species: closed (POSS) or open (OPOSS) cages, ladder (LSSQ) or random (RSSQ) structures. According to established data in literature [34,35], in tetrahedral SiO_2, the Si-O-Si bond angle is 144°, and the Si-O asymmetric stretch band position is at 1080 cm^{-1}. In ordered LSSQ structures, the band is shifted to around 1150 cm^{-1}, while in more cage-like structures, the Si-O-Si bond angles open to 150° or greater, and the Si-O-Si band position shifts to higher frequency, sometimes as high as ~1180 cm^{-1}. In more network-like structures, the bond angle reduces to <144° and the Si-O peak position shifts downward in energy, to ~1030 cm^{-1} [33,36]. In our case, it seems that most of these species co-exist proved by the absorption bands at 1145 cm^{-1} (LSSQ), 1167 cm^{-1} (OPOSS) and 1190 cm^{-1} (POSS), that are more or less displaced from those indicated in the literature by various authors. The strong band at 480 cm^{-1} is assigned to Si-O-Si symmetric bending. All these indicate formation of silsesquioxane structures within the polydimethylsiloxane matrix. The hydrogen-bonded silanol groups that could belong to OPOSS, LSSQ or RSSQ are observed at 3416, 3478 and 3557 cm^{-1}, while a band at 912 cm^{-1} is assigned to Si-OH bending. The Si-CH_3 bending is at 1263 cm^{-1} while Si-C stretching is at 800 cm^{-1}. The bands around 1400 (1410 and 1443 cm^{-1}) come from asymmetric deformations of C-H in propyl group [33]. The band at 644 is assigned to CH_2-Cl [37]. In the spectrum of A_5-G sample where, as would be expected according to the amount of added CPTMS,

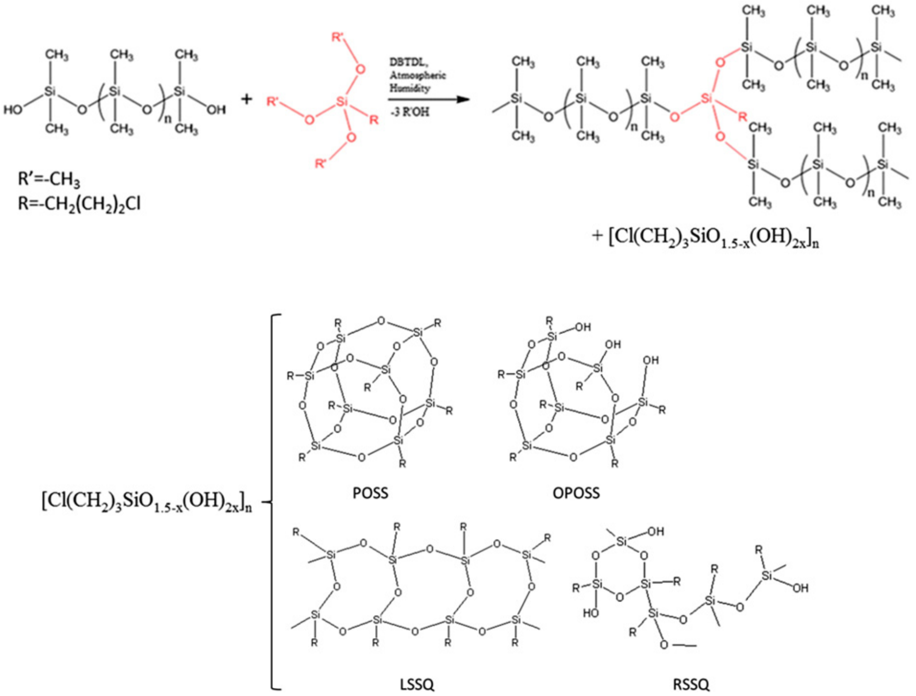

Scheme 1. Reaction leading to PDMSs cross-linking and their *in situ* filling with a polar component, **Cl-propyl-SSQ**; (**Cl-propyl-SSQ** could be closed (POSS) or open (OPOSS) cages, ladder (LSSQ) or random (RSSQ) structures [31]; excepting the first one, all of them possess Si-OH groups.

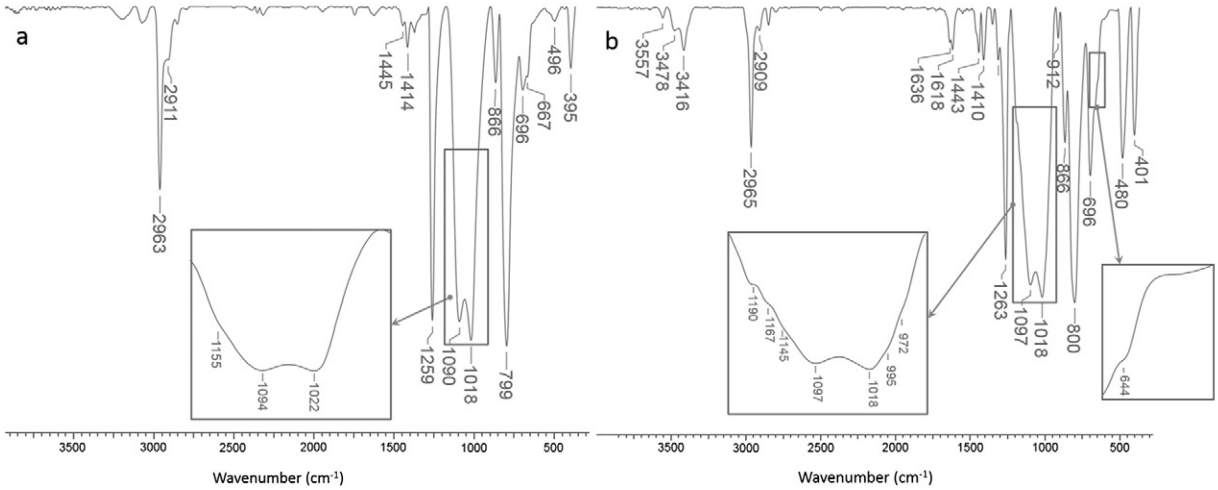

Fig. 1. IR spectra exemplified for the samples A_5-G (a) and A_{50}-G (b); insets are details for the spectral region 1225–930 cm^{-1} with the overlapped SSQ bands indicated by arrows.

silsesquioxane species are in smaller quantities, these shoulders or bands cannot be identified they being almost completely covered by the bands of the silicone matrix (Fig. 1a).

3.2. TEM analysis

Model samples, A_5-G, A_{15}-G and A_{50}-G consisting in mixtures based on polydimethylsiloxane end-blocked with trimethylsiloxy groups, instead of crosslinkable polydimethylsiloxane-α,ω-diols, and hydrolysis-condensation products of 5, 15 and 50 wt% added CPTMS, processed in similar conditions (exposure to atmospheric humidity, catalyst) to A series, have been prepared for TEM imaging. This approach was selected since it provides the best solution to get to the internal morphology of the material. Tentative to cut the solid films produced artefacts that obscured the real arrangements of the SSQ nanoparticles within the soft polysiloxane matrix. The obtained mixtures, with consistence between fluid and solid, can be easily transferred onto the TEM grids without affecting their internal morphology. For a certain concentration of the components, the structure is stable enough to draw conclusions concerning interactions of the components and evolution of the system

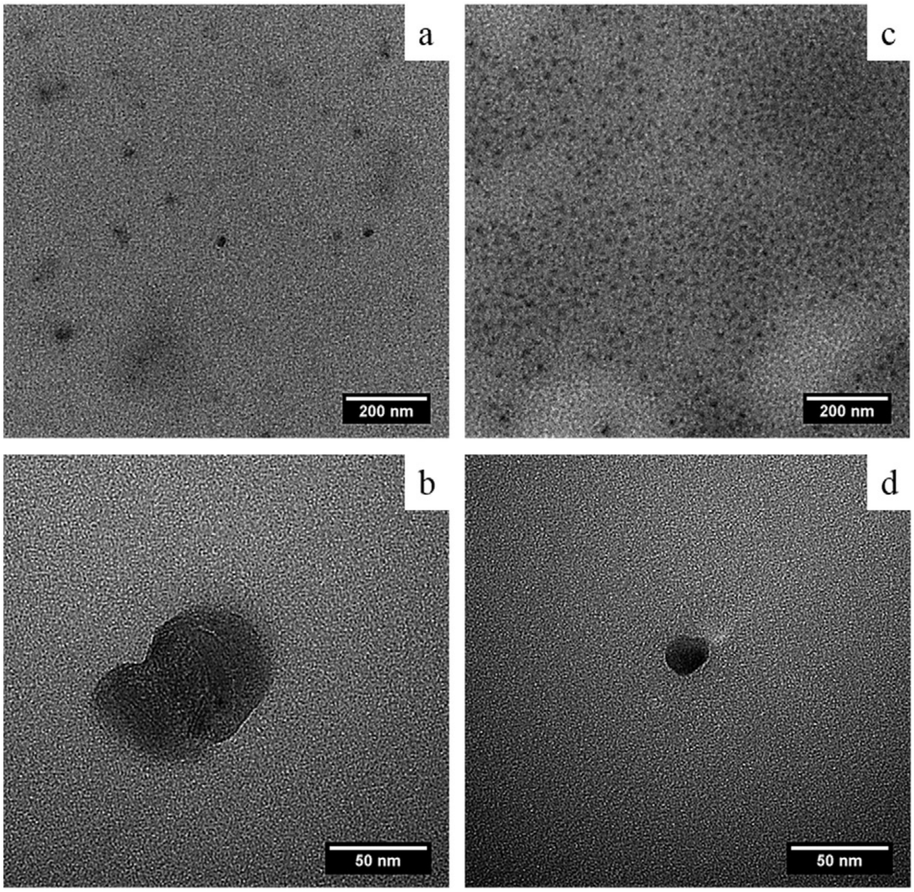

Fig. 2. TEM images of model samples A_{15}-G (a, b) and A_{50}-G (c, d) showing the presence of filler.

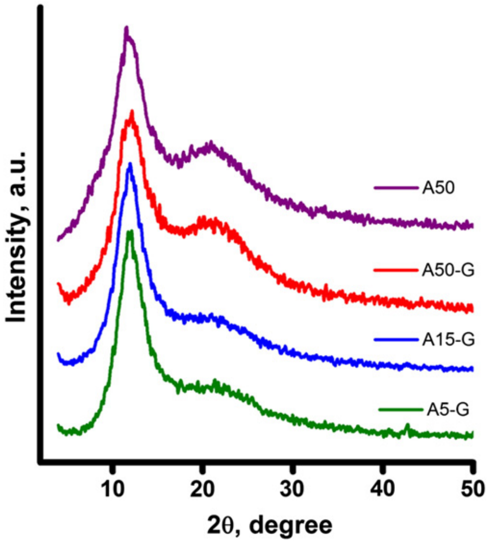

Fig. 3. Normalized WAXD spectra of silicone oil-CPTMS samples, A_5-G, A_{10}-G and A_{50}-G as well as of the crosslinked film, A_{50}.

toward their particular distribution or spatial arrangements. Thus, as can be observed in Fig. 2, nanostructures of a few tens nanometer (20–50 nm) size are embedded within the soft matrix, and these are the more frequent as the amount of added CPTMS is higher (sample A_{50}-G). These nanostructures possess a sphere-like shape probably adopted to minimize the contact surface between polar chloropropylsilsesquioxane structures and nonpolar dimethylsiloxane matrix.

3.3. X-ray analysis

The WAXD spectra recorded for some of our samples, both in model mixtures and cross-linked films are comparatively presented in Fig. 3. Two characteristic diffraction peaks were reported for ladder phenylsilsesquioxane (Phenyl-LSSQ), a sharp one at 7.3° and a diffuse one at 18.8°, assigned to the intramolecular periodic chain-to-chain distance (12.1 Å) and the average thickness of the amorphous LSSQ, respectively (4.7 Å) [38]. The diffractograms obtained for our samples indicate semi-crystalline materials, with a diffraction peak around 12° (2θ), corresponding to d spacing values (chain-to-chain distance) of around 7.3 Å and an amorphous halo centered at around 22° (2θ), which would correspond to a LSSQ thickness of around 4 Å. Based on molecular modelling, the average distance between the siloxane chains in a LSSQ is indeed around 4 Å, while the lengths of the lateral chloropropyl substituent is 5.5 Å (Fig. S1). Due to the polar nature of the Cl groups, the periodic chain-to-chain distance should be less than double this value (interdigitated assembling), thus the found distance of 7.3 Å is reasonable. We did not find data for chloropropyl-LSSQ, but based on the presence of similar diffraction pattern, we presume that ladder-like structures are mainly formed. This would be in agreement with IR results, where the most intense “SSQ” band was at 1145 cm^{-1}, assigned to LSSQ. However, based on WAXD we cannot exclude the presence of other species with diffraction maxima enveloped under the amorphous halo.

Further investigations have been performed with the purpose to evidence nanostructured SSQ phase in crosslinked silicone thin film A_{50} by SAXS technique. SAXS analysis of the simple silicone thin film was used to obtain the background that was further subtracted to correct the data. The scattering curve in log-log plot (Fig. 4a) shows the correlation peak located within the low q values range. This confirms the presence of strong physico-chemical interactions between the nanostructures within the silicon matrix. The Lorentz-corrected scattering curve (Fig. 4b) indicates that these are long distance interactions having the long period L = 22 nm. Analysis of the polymeric matrix (polydimethylsiloxane-α,ω-diols) as a reference sample prepared without addition of SSQ precursor did not show any characteristic peaks within the measured q range. Therefore, it is obvious that the presence of the nanostructured SSQ phase is the main cause. The long range period represents the average thickness of the layer where both the crystalline and amorphous phases coexist. Such a nanostructuration of the material could be the result of a lamellar morphology that occurs by SSQ particles self-assembling into the amorphous PDMS matrix. Lack of the higher order reflections should be a consequence of aggregates dispersion within the matrix. However, the ordering degree found in non-crosslinked samples, A_5 and A_{15}-G, is higher (Figs. S2 and S3) due to the high mobility of phases, which allows the aggregation of the SSQ nanostructures with lower long range periods (L).

3.4. Stress-strain measurements

After aging, the mechanical behavior of the cross-linked films was evaluated by tensile testing. As the stress-strain curves indicate (Fig. 5), *in situ* generated, partially or totally condensed cage-like structures or networks act as fillers for polydimethylsiloxane matrix. The Young's modulus slightly increased in both series with the amount of CPTMS added. However, all samples have modulus values below 1 MPa, except A_{50} and B_{50} with 2.54 and 1.83 MPa, respectively (Table 2). The effect of this filler is emphasized by the shape of the stress-strain curves. As a general trend, the tensile strength increased with the amount of CPTMS added, while the maximum strain decreased. However, in both series, the strain registered a minimum for about 5% and a maximum at about 15% CPTMS added. The reason for this might be

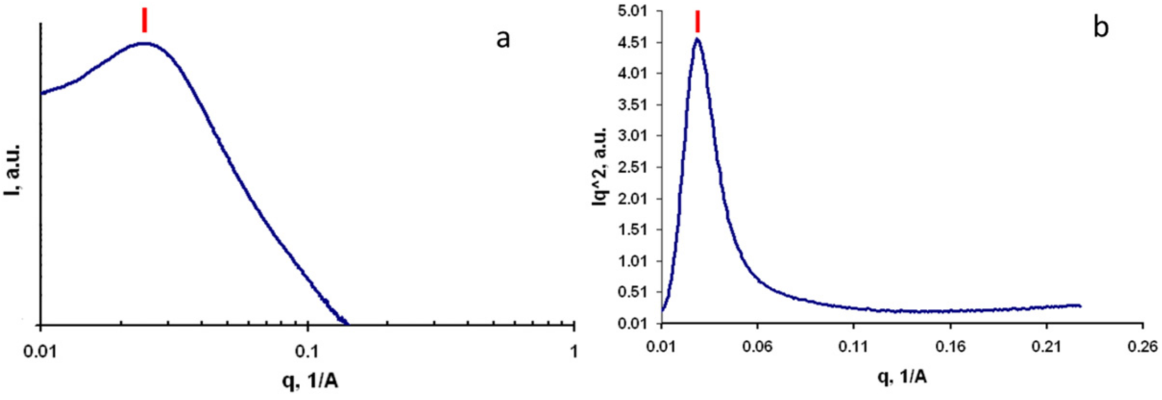

Fig. 4. SAXS results for A_{50} sample: a — Scattering curve (log-log plot) showing the presence of a correlation peak; b — Lorentz-corrected scattering curve.

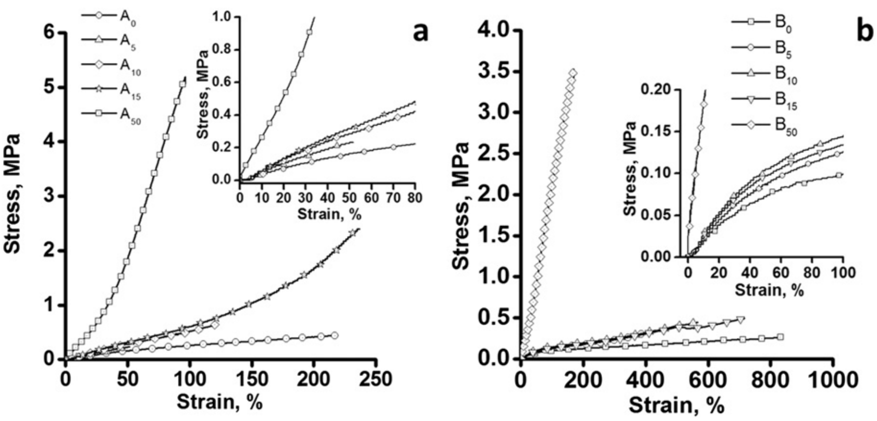

Fig. 5. Uniaxial stress-strain curves for A and B series.

Table 2
The main mechanical and dielectric characteristics.

Sample	T_{nm},[a] MPa	S_m,[b] %	Y,[c] MPa	ε′,[d] 1 Hz	ε″,[e] 1 Hz	ε′,[d] 100 Hz	ε″,[e] 100 Hz	Ebs[f], V/μm	S_e,[g] %
A_0	0.44	218	0.32	3.94	11.27	3.17	0.14	55.57	5.96
A_5	0.23	51	0.41	9.01	67.06	3.21	0.77	44.19	3.70
A_{10}	0.64	122	0.51	6.56	46.37	3.36	0.53	62.16	5.43
A_{15}	2.39	236	0.55	4.92	18.95	3.71	0.21	56.00	7.08
A_{50}	5.05	97	2.54	4.31	25.25	3.48	0.26	35.17	1.39
B_0	0.26	835	0.19	7.06	19.50	2.75	0.28	35.71	4.17
B_5	0.31	395	0.18	5.79	31.30	3.35	0.36	48.98	7.29
B_{10}	0.44	566	0.23	4.00	9.90	3.15	0.12	44.74	5.96
B_{15}	0.49	716	0.21	4.06	4.63	3.47	0.05	40.00	5.30
B_{50}	3.42	169	1.83	4.50	15.66	3.52	0.18	46.67	2.08

a – mechanical stress, nominal; b – mechanical strain; c – Young's modulus (at 10% strain); d – dielectric permittivity; e – dielectric loss; f –electrical breakdown strength in actuator; g – maximum measured actuation strain.

the different shape of the SSQ aggregates/particles formed, besides their amount and possible different condensation degree within the cross-linked matrix. A very large amount (~50%) of CPTMS leads to increased stiffness of the resulted films. Comparing the two series, it is obvious that series B provided materials with much better mechanical properties. The maximum strain decreased in B series from 835% for B_0 to 395% for B_5, and down to 169% for B_{50}. The same trend is observed for A series but, due to the lower molecular weight of the PDMS matrix, the maximum strain for A_0 was only 218%, and decreases with addition of CPTMS, down to 51% for A_5 and to 97% for A_{50}. As mentioned before, the best mechanical properties were obtained by addition of around 15% CPTMS, *i.e.* maximum strains of 716% for B_{15} and 236% for A_{15} and low Young modulus.

3.5. Dielectric measurements

The dielectric spectra of the samples were recorded in the range of 1 Hz–1 MHz (Figs. 6 and 7). High ε′and ε″ values are observed for both series at low frequencies and surprisingly, there is not a direct correlation between them and samples composition. As it is well known, this increase is attributed to interfacial polarization, due to the accumulation of charges at interfaces with different conductivities. As TEM and X-ray analyses showed, the samples present complex multiphase morphology consisting of amorphous and crystalline domains, the last being different inorganic SSQ nanostructurs. Consequently, there is an interfacial polarization due to multiphase morphology besides polarization at the electrode – polymer interface. However, when we compare the data for frequencies higher than about 100 Hz, where the dipolar polarization prevails, there is a good correlation between the increase of dielectric constant and the estimated amount of polar groups (Table 1). Thus, as expected, the permittivity increases with the amount of CPTMS added, from 3.17 and 2.75 (at 100 Hz) for reference samples, A_0 and B_0, up to 3.48 and 3.52 for corresponding samples with around 50% CPTMS added, at the same frequency (Table 2). The difference between the two samples can be explained by the different cross-linking density. Because the cross-linking used is condensative one, which is made by linking the polysiloxane chain ends with a trifunctional agent, the crosslinking density is lower when the chains are longer, as in series B. As a result, the free volume is higher leading to a low value of the dielectric permittivity in the case of sample B_0 as compared with sample A_0 having lower molecular weight. On the other hand, we have to keep in mind that the samples are cross-linked with the polar silane, thus the smaller the chains are, the higher is the proportion of Cl into the mass unit, for example, sample A_0 contains 4 times more Cl

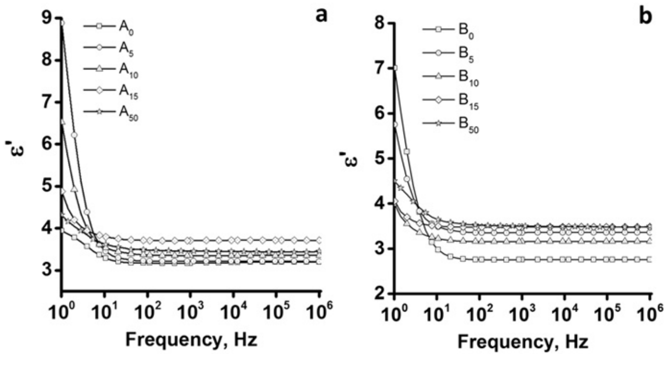

Fig. 6. Variation of the dielectric permittivity, ε′, in dependence on frequency for the two series of samples.

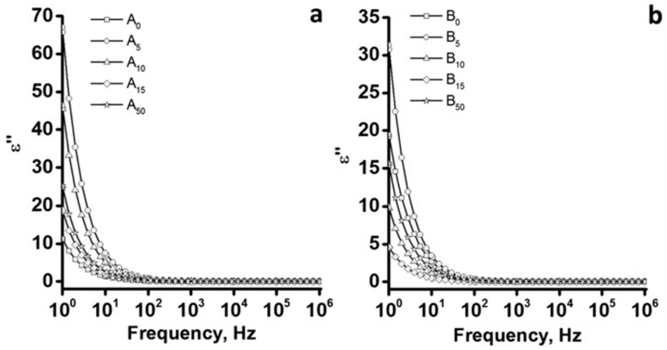

Fig. 7. Variation of the dielectric losses, ε″, depending on the frequency for the two series of samples.

than sample B_0, which is reflected in the increased ε′. All values for dielectric loss generally remain low at high frequency (Fig. 7). The dipole content was calculated reported to the total weight, assuming complete conversion of CPTMS. The ε′ value at 100 Hz increases only slightly with raising the chloro content up to around 10.587, while the Young's modulus significantly increases (Table 2, Fig. S4). Compared with literature [39], when the same dipole was used but attached on the backbone of PDMS (29,000 $g \cdot mol^{-1}$), for almost the same amounts of dipole (roughly 1.35 and 2.70 wt% Cl), our samples A_{10}, A_{15} containing 1.78 and 2.52 wt% Cl and B_{10}, B_{15} with 1.70 and 2.48 wt% Cl show lower ε′ values (3.36/3.71 and 3.15/3.47 compared with 3.9 and 4.4 at 100 Hz) but also lower Young's modulus values (0.23 and 0.21 compared with 2.8 and 1.5 MPa), which could be an advantage regarding their use for actuation. These differences occur because different cross-linking pathways were used. On the other hand, higher ε′ obtained in the case of chloropropyl-modified polysiloxanes could be due to more freedom in dipole orientation in the electric field, compared to limited mobility in SSQ clusters. The sample A_0 with a dense network, and as a result a low free volume, shows higher value for electrical breakdown strength, Ebs (55.57 V/μm), as compared with value recorded for low cross-linked B_0 sample (35.71 V/μm) (Table 2, Fig. S4). Instead, it is difficult to identify a pattern of variation of this feature in the two series with increasing the amount of CPTMS added. This is due to complication of system as a result of the formation of silsesquioxane structures with varying degrees of condensation and their involvement in the crosslinking process. However, these values remain reasonable in practical terms.

3.6. Electromechanical measurements

The deformation (thickness reduction and area expansion) capacity of the dielectric films under the action of the electric field, known as electrical actuation, was measured by applying a voltage with an increasing rate of 100 V every 2 s on the film samples. The lateral strain curves are showed in Fig. 8, while the maximum lateral strain, S_e, values are centralized in Table 2. Two of the main material characteristics that determine this function are dielectric permittivity and Young modulus [40,41], which we have tried to manipulate through this approach. As can be seen, the sample A_0 shows higher lateral strain value (5.96%) as compared with B_0 (4.17%). By incorporating ascending amounts of CPTMS, which generates polar filler within polysiloxane matrix having different molecular masses, modifications of this characteristic are recorded in dependence on the balance between values of the two parameters, antagonistically acting on it (Fig. S4). So, while dielectric permittivity should be high, the modulus should be rather lower one. In our case, on the one hand, the amount of SSQ filler *in situ* formed should increase both modulus by reinforcing and the dielectric permittivity due to polar groups brought with it. On the other hand, crosslinking density, dictated by the chains length of the matrix polymer, when these are short, should result in a dense network with higher modulus and as a consequence in increased dielectric permittivity due to low free volume and high density of dipoles in the cross-linking knots. Given the complexity of this dependency, it requires an optimization study which we hope to make the subject of our future work. In both series, the lowest values for the actuation strain, even smaller than the reference samples, were obtained for samples with around 50 wt% added CPTMS, 1.39 and 2.08% for the samples A_{50} and B_{50}, respectively, due to much higher Young's modulus which is not compensated by the small increase of ε'. The best values for lateral strain were recorded on the samples A_{15} (7.08%) and B_5 (7.29%).

In Fig. 9, the measured actuation values are presented in parallel with those of electromechanical sensitivity, the latter being calculated based on both parameters of interest for electromechanical response, ε′ and Young's modulus. For a better comparison between samples, the actuation values were read on the curve at a voltage of 33 V/μm, which is the highest voltage that all samples withstand. In both series, the trends for the two parameters are roughly the same except for the sample B_5; although it has the highest value for electromechanical sensitivity, the actuation value at 33 V/μm is slightly smaller even than the sample B_0. Note however that this sample has the lowest value for the Young's modulus, 0.18 MPa, and the highest value for actuation at its breakdown, 7.29% at 48.98 V/μm (Table 2). As expected, series B

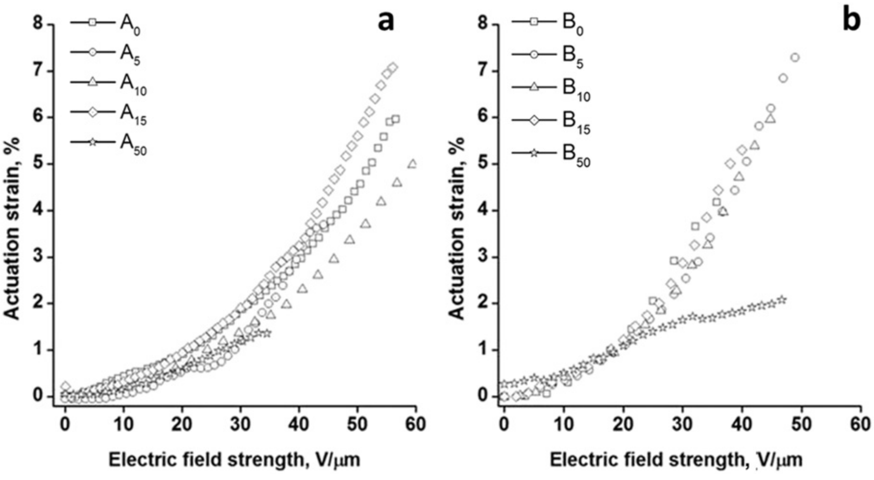

Fig. 8. Actuation strain curves for: a – A series; b – B series.

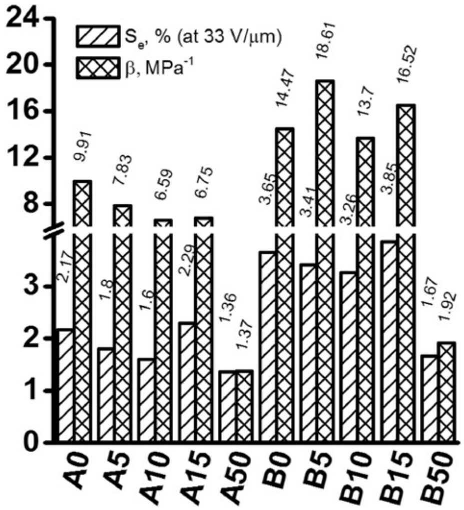

Fig. 9. Comparative presentation of measured actuation strain values at 33 V/μm and theoretical estimated electromechanical sensitivities, β (MPa^{-1}), calculated as a ratio between ε′ and Young's modulus at 10% strain.

samples show higher values compared to series A, both for sensitivity and electromechanical actuation. The maximum actuation has an increasing trend *versus* the electromechanical sensitivity (Fig. S5).

One of the two samples with around 15% added CPTES which proved to have good values both for dielectric strength (56 kV/μm) and actuation (7.08%), namely A_{15} was chosen for the study of electro-mechanical fatigue resistance, by cyclic tests applying a voltage of 5600 V. The results are presented in comparison with those obtained in the same reference sample A_0 (Fig. 10). None of the two elastomers was damaged after 100 cycles.

4. Conclusions

Two series of silicone films based on two PDMSs with different molecular masses were prepared by condensative cross-linking with CPTMS incorporated in stoichiometric amounts (samples A_0 and B_0) or in increasing weight percentages of around 5, 10, 15 and 50 wt% reported to the mixture weight (samples A_5–A_{50} and B_5–B_{50}). The conversion of the CPTMS excess in silsesquioxane structures was emphasized by FTIR by the presence of characteristic absorption bands, while their ordering and aggregation within the silicone matrix was emphasized by TEM, WAXD and SAXS. The effects of the dipole content brought by CPTMS addition as well as the molecular weight of host matrix were evaluated in terms of mechanical, dielectric and electro-mechanical characteristics. The results have shown that with increasing the content in polar groups (in line with CPTMS amount used), a slight increase in dielectric permittivity (3.17–3.48 in A series and 2.75–3.52 in B series) and a more pronounced increase of the Young's modulus (0.32–2.54 in A_0–A_{50} series and 0.19–1.83 in B_0–B_{50} series) were registered. The increase of molecular weight of the used PDMS mainly results in lowering the Young's modulus. The dielectric strength randomly ranged between 35.17–62.16 V/μm, the highest values being within A series, while the lateral strain value varied between 1.39–7.29%, the highest values being recorded on the samples A_{15} (7.08%) and B_5 (7.29%). Although these values are not spectacular, it can be appreciated that by using CPTMS as both cross-linker and precursor for polar filler the electromechanical performance of the polydimethylsiloxane is easily improved, without involving a complex chemistry.

Acknowledgements

We gratefully acknowledge the financial support of Swiss National Science Foundation and UEFISCDI, under the Swiss-Romanian Cooperation Program, grant No. IZERZO_142215/1 (10/RO-CH/RSRP/01.01.2013). Actuation measurements were performed in Laboratory for Functional Polymers (Dr. D. Opris), Empa, Swiss Federal Laboratories for Materials Science and Technology, Dübendorf, Switzerland for which we address warm thanks.

Appendix A. Supplementary data

Supplementary data to this article can be found online at http://dx.doi.org/10.1016/j.matdes.2016.06.010.

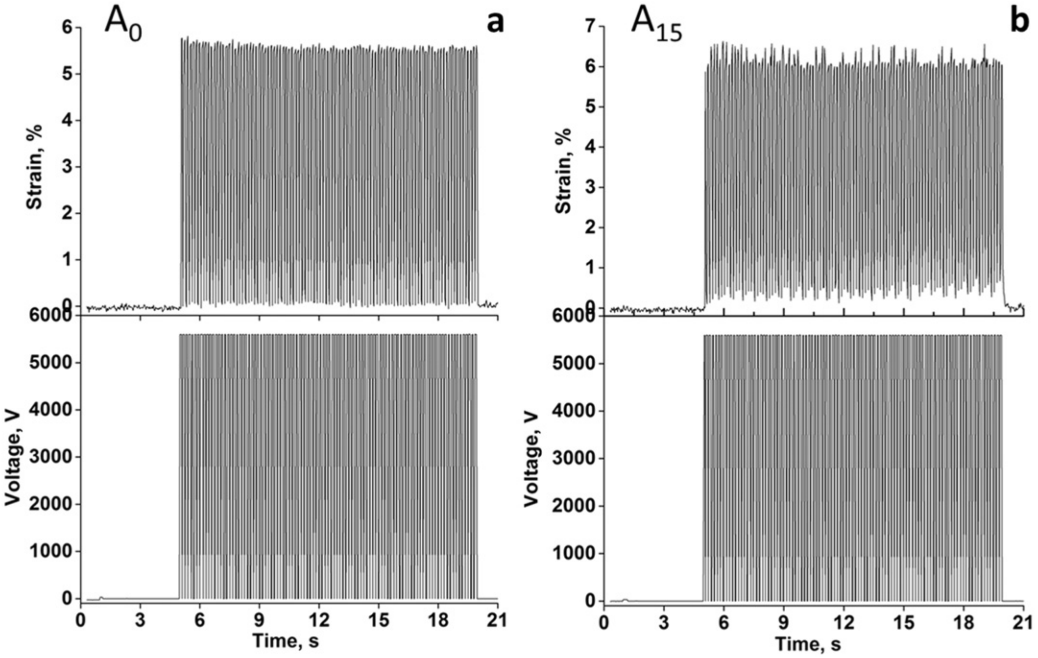

Fig. 10. Illustrative representation of electro-mechanical fatigue resistance for sample A_{15} (b), as compared with reference A_0 (b), at a cyclic applying of 5600 V.

References

[1] W. Noll, Chemistry and Technology of Silicone, Academic Press, Orlando, 1968.

[2] A. Colas, Silicones: preparation, properties and performance. Dow corning: life sciences, http://www.dowcorning.com/content/publishedlit/01-3077.pdf.

[3] F. Carpi, G. Gallone, F. Galantini, D. De Rossi, Enhancing the dielectric permittivity of elastomers, in: F. Carpi, D. De Rossi, R. Kornbluh, R. Pelrine, P. Sommer-Larsen (Eds.), Dielectric Elastomers as Electromechanical Transducers: Fundamentals, Materials, Devices, Models and Applications of an Emerging Electroactive, Polymer Technology, Elsevier Ltd. 2008, pp. 51–68.

[4] J.A. Clarson, J.A. Semlyen, Siloxane Polymers, Englewood Cliffs: Prentice Hall, 1993.

[5] M.R. Ramli, M.B.H. Othman, A. Arifin, Z. Ahmad, Cross-link network of polydimethylsiloxane via addition and condensation (RTV) mechanisms. Part I: synthesis and thermal properties, Polym. Degrad. Stab. 96 (2011) 2064–2070, http://dx.doi.org/10.1016/j.polymdegradstab.2011.10.001.

[6] Y.T. Looi, R. Ramli, M.B.H. Othman, A. Zulkifli, Synthesis and characterization of highly cross-link polysiloxane based on 2,4,6,8-tetramethyl-2,4,6,8-tetravinylcyclotetrasiloxane, Adv. Mater. Res. 295-297 (2011) 2393–2395 (10.4028/www.scientific.net/AMR.295-297.2393).

[7] J. Heiner, B. Stenberg, M. Persson, Crosslinking of siloxane elastomers, Polym. Test. 22 (2003) 253–257, http://dx.doi.org/10.1016/S0142-9418(02)00081-8.

[8] Z. Wang, A.A. Volinsky, N.D. Gallant, Crosslinking effect on polydimethylsiloxane elastic modulus measured by custom built compression instrument, J. Appl. Polym. Sci. 131 (2014) 41050, http://dx.doi.org/10.1002/app.41050.

[9] D.M. Opris, M. Molberg, C. Walder, Y.S. Ko, B. Fischer, F.A. Nüesch, New silicone composites for dielectric elastomer actuator applications in competition with acrylic foil, Adv. Funct. Mater. 21 (2011) 3531–3539, http://dx.doi.org/10.1002/adfm.201101039.

[10] B. Kussmaul, S. Risse, M. Wegener, G. Kofod, H. Krüger, Matrix stiffness dependent electro-mechanical response of dipole grafted silicones, Smart Mater. Struct. 21 (2012) 064005, http://dx.doi.org/10.1088/0964-1726/21/6/064005 (6 pp.).

[11] S. Risse, B. Kussmaul, H. Krüger, G. Kofod, Synergistic improvement of actuation properties with compatibilized high permittivity filler, Adv. Funct. Mater. 22 (2012) 3958–3962, http://dx.doi.org/10.1002/adfm.201200320.

[12] F.B. Madsen, I. Dimitrov, A. Daugaard, S. Hvilsted, A.L. Skov, Novel cross-linkers for PDMS networks for controlled and well distributed grafting of functionalities by click chemistry, Polym. Chem. 4 (2013) 1700–1707, http://dx.doi.org/10.1039/c2py20966g.

[13] C. Racles, M. Cazacu, B. Fischer, D.M. Opris, Synthesis and characterization of silicones containing cyanopropyl groups and their use in dielectric elastomer actuators, Smart Mater. Struct. 22 (2013) 104004, http://dx.doi.org/10.1088/0964-1726/22/10/104004 (10 pp.).

[14] C. Racles, M. Alexandru, A. Bele, V. Musteata, M. Cazacu, D.M. Opris, Chemical modification of polysiloxanes with polar pendant groups by co-hydrosilylation, RSC Adv. 4 (2014) 37620–37628, http://dx.doi.org/10.1039/c4ra06955b.

[15] B. Kussmaul, S. Risse, M. Wegener, M. Bluemke, J. Krause, J. Wagner, T. Feller, K. Clauberg, J. Hitzbleck, R. Gerhard, H. Kruege, in: Y. Bar-Cohen (Ed.), New DEA Materials by Organic Modification of Silicone and Polyurethane Networks in SPIE Electroactive Polymer Actuators and Devices (EAPAD) 2013, 8687 2013, p. 86872S.

[16] C. Racles, A. Bele, M. Dascalu, V.E. Musteata, C.D. Varganici, D. Ionita, S. Vlad, M. Cazacu, S.J. Dünki, D.M. Opris, Polar–nonpolar interconnected elastic networks with increased permittivity and high breakdown fields for dielectric elastomer transducers, RSC Adv. 5 (2015) 58428–58438, http://dx.doi.org/10.1039/c5ra06865g.

[17] A. Hisyam, A. Razak, P. Szabo, A.L. Skov, Enhancement of dielectric permittivity by incorporating PDMS-PEG multiblock copolymers in silicone elastomers, RSC Adv. 5 (2015) 53054–-58428, http://dx.doi.org/10.1039/c5ra09708h.

[18] L. Yu, F.B. Madsen, S. Hvilsted, A.L. Skov, Dielectric elastomers with very high dielectric permittivity, based on silicone and ionic interpenetrating networks, RSC Adv. 5 (2015) 49739–49747, http://dx.doi.org/10.1039/C5RA07375H.

[19] G. Gallone, F. Carpi, D. De Rossi, G. Levita, A. Marchetti, Dielectric constant enhancement ina silicone elastomer filled with lead magnesium niobate-lead titanate, Mater. Sci. Eng. C 27 (2007) 110–116, http://dx.doi.org/10.1016/j.msec.2006.03.003.

[20] H. Zhao, D.R. Wang, J.W. Zha, J. Zhao, Z.M. Dang, Increased electroaction through a molecular flexibility tuning process in TiO_2–polydimethylsilicone nanocomposites, J. Mater. Chem. A 1 (2013) 3140, http://dx.doi.org/10.1039/c2ta01026g.

[21] W. Hu, S.N. Zhang, X. Niu, C. Liu, Q. Pei, Aluminum nanoparticle/acrylate copolymer nanocomposites for dielectric elastomers with high dielectric constants, in: Y. Bar-Cohen (Ed.), SPIE Smart Structures and Materials + Nondestructive Evaluation and Health Monitoring, 9056, 2014, 90561Ohttp://dx.doi.org/10.1117/12.2045049.

[22] A. Bele, G. Stiubianu, C. Varganici, M. Ignat, M. Cazacu, Silicone dielectric elastomers based on radical crosslinked high molecular weight polydimethylsiloxane co-filled with silica and barium titanate, J. Mater. Sci. 50 (2015) 6822–6832, http://dx.doi.org/10.1007/s10853-015-9239-y.

[23] G. Stiubianu, A. Bele, M. Cazacu, C. Racles, S. Vlad, M. Ignat, Dielectric silicone elastomers with mixed ceramic nanoparticles, Mater. Res. Bull. 71 (2015) 67–74, http://dx.doi.org/10.1016/j.materresbull.2015.07.005.

[24] A. Bele, M. Cazacu, G. Stiubianu, S. Vlad, Silicone-barium titanate composites with increased electromechanical sensitivity. The effects of the filler morphology, RSC Adv. 4 (2014) 58522–58529, http://dx.doi.org/10.1039/c4ra09903f.

[25] A. Bele, M. Cazacu, G. Stiubianu, S. Vlad, M. Ignat, Polydimethylsiloxane-barium titanate composites: preparation and evaluation of the moisture, thermal, mechanical and dielectric behavior, Comp. Part B 68 (2015) 237–245, http://dx.doi.org/10.1016/j.compositesb.2014.08.050.

[26] M. Cazacu, M. Ignat, C. Racles, M. Cristea, V. Musteata, D. Ovezea, D. Lipcinski, Well-defined silicone-titania composites with good performances in actuation and energy harvesting, J. Compos. Mater. 48 (2014) 1533–1545, http://dx.doi.org/10.1177/0021998313488148.

[27] F.B. Madsen, A.E. Daugaard, S. Hvilsted, A.L. Skov, The current state of silicone-based dielectric elastomer transducers, Macromol. Rapid Commun. 37 (2016) 378–413, http://dx.doi.org/10.1002/marc.201500576.

[28] F.B. Madsen, A.E. Daugaard, S. Hvilsted, M.Y. Benslimane, A.L. Skov, Dipolar cross-linkers for PDMS networks with enhanced dielectric permittivity and low dielectric loss, Smart Mater. Struct. 22 (2013) 104002, http://dx.doi.org/10.1088/0964-1726/22/10/104002 (11 pp.).

[29] A. Bele, M. Cazacu, C. Racles, G. Stiubianu, D. Ovezea, M. Ignat, Tuning the electromechanical properties of silicones by crosslinking agent, Adv. Eng. Mater. 17 (2015) 1302–1312, http://dx.doi.org/10.1002/adem.201400505.

[30] M. Cazacu, M. Marcu, Contributions to polydimethylsiloxane-α,ω-diol synthesis by heterogeneous catalysis, Macromol. Rep. A 32 (1995) 1019–1029, http://dx.doi.org/10.1080/10601329508019142.

[31] G. Kickelbick, Silsesquioxanes, Struct. Bond. 155 (2014) 1–28, http://dx.doi.org/10.1007/430_2013_108.

[32] P.J. Launer, Infrared analysis of organosilicon compounds: spectra-structure correlations, in: R. Anderson, B. Arkles, G. Larson (Eds.), Silicone Compounds Register and Review, 4th edition S-7Inc. Bristol: Petrarch Systems 1987, pp. 100–103.

[33] H. FI, H. LH, J. Gorecki, D.".A. L., Silsesquioxanes as precursors to ceramic composites, Silsesquioxanes as Precursors to Ceramic Composites, NASA Technical Memorandum 89893, 11th Annual Conference on Composites, Advanced Ceramics and Composite Materials, Florida, 1987 (January 18–23).

[34] G. Lucovsky, M.J. Mantini, J.K. Srivastava, E.A. Irene, Low-temperature growth of silicon dioxide films: a study of chemical bonding by ellipsometry and infrared spectroscopy, J. Vac. Sci. Technol. B 5 (1987) 530, http://dx.doi.org/10.1116/1.583944.

[35] Y.H. Kim, M.S. Hwang, H.J. Kim, J.Y. Kim, Y. Lee, Infrared spectroscopy study of low-dielectric-constant fluorine-incorporated and carbon-incorporated silicon oxide films, J. Appl. Phys. 90 (2001) 3367–3370, http://dx.doi.org/10.1063/1.1402152.

[36] P.G. Pai, S.S. Chao, Y. Takagi, G. Lucovsky, Infrared spectroscopic study of SiO_x films produced by plasma enhanced chemical vapor deposition, J. Vac. Sci. Technol. A 4 (1986) 689, http://dx.doi.org/10.1116/1.573833.

[37] J.J. Shipman, V.L. Folt, S. Krimm, Characteristic infrared frequencies of rotational isomers of alkyl chlorides, Spectrochim. Acta 18 (1962) 1603, http://dx.doi.org/10.1016/0371-1951(62)80024-1.

[38] S.S. Choi, A.S. Lee, S.S. Hwang, K.Y. Baek, Structural control of fully condensed polysilsesquioxanes: ladderlike vs cage structured polyphenylsilsesquioxanes, Macromolecules 48 (2015) 6063–6070, http://dx.doi.org/10.1021/acs.macromol.5b01539.

[39] F.B. Madsen, L. Yu, A.E. Daugaard, S. Hvilsted, A.L. Skov, Dielectric elastomers, with very high dielectric permittivity, based on silicone and ionic interpenetrating networks, RSC Adv. 5 (2015) 10254–10259, http://dx.doi.org/10.1039/C5RA07375H.

[40] R.E. Pelrine, R.D. Kornbluh, J.P. Joseph, Electrostriction of polymer dielectrics with compliant electrodes as a means of actuation, Sensors Actuators A Phys. 64 (1998) 77–85, http://dx.doi.org/10.1016/S09244247(97)01657-9.

[41] P. Brochu, Q. Pei, Advances in dielectric elastomers for actuators and artificial muscles, Macromol. Rapid Commun. 31 (2010) 10–36, http://dx.doi.org/10.1002/marc.200900425.